

Numerical Solutions of the Lane-Emden Equation and Stellar Density Profiles



Sepand Khosravi

Department of Physics and Energy Engineering, Amirkabir University of Technology,
No. 424 Hafez Ave., Tehran, Iran.

ISSN 1870-9095

E-mail: sepandkhosravi1@gmail.com

(Received 3 November 2025, accepted 18 December 2025)

Abstract

We present numerical solutions of the Lane-Emden equation for selected polytropic indices using a fourth order Runge-Kutta integrator with series expansion initial conditions. The method is validated against the analytical cases $n = 0$ and $n = 1$, then applied to the astrophysically relevant indices $n = 1.5$ and $n = 3$. The computed first zeros are $\xi_1 \approx 3.654$ ($n = 1.5$) and $\xi_1 \approx 6.897$ ($n = 3$), and the resulting density profiles show that increasing n produces more extended, less centrally concentrated models. The $n = 3$ polytropic model yields a solar radius of the correct order of magnitude, showing that even a simplified pressure-density relation can capture the essential structural scaling of real stars like the Sun.

Keywords: Lane-Emden equation, Polytropes, Stellar structure.

Resumen

Presentamos soluciones numéricas de la ecuación de Lane-Emden para índices politrópicos seleccionados utilizando un integrador Runge-Kutta de cuarto orden con condiciones iniciales de expansión en serie. El método se valida frente a los casos analíticos $n = 0$ y $n = 1$, y posteriormente se aplica a los índices astrofísicamente relevantes $n = 1.5$ y $n = 3$. Los primeros ceros calculados son $\xi_1 \approx 3.654$ ($n = 1.5$) y $\xi_1 \approx 6.897$ ($n = 3$), y los perfiles de densidad resultantes muestran que al aumentar n se obtienen modelos más extendidos y con menor concentración central. El modelo politrópico $n = 3$ proporciona un radio solar del orden de magnitud correcto, lo que demuestra que incluso una relación presión-densidad simplificada puede capturar la escala estructural esencial de estrellas reales como el Sol.

Palabras clave: Ecuación de Lane-Emden, Politropos, Estructura estelar.

I. INTRODUCTION

One of the most fundamental equations describing stellar structure is the Lane-Emden equation, which characterizes the dimensionless density profile of a spherically symmetric star in hydrostatic equilibrium with a pressure-density relation defined by a polytropic index [1, 2]. Hypothetical stellar models in which the pressure depends on the density in the form

$$P = K \rho^{\frac{n+1}{n}}, \quad (1)$$

are known as polytropes, where K is a constant and n is the polytropic index [1].

The starting point for deriving the Lane-Emden equation is the condition of hydrostatic equilibrium [1],

$$\frac{dP}{dr} = -G \frac{dM(r)\rho}{r^2}, \quad (2)$$

together with the mass continuity equation [1],

$$\frac{dM}{dr} = 4\pi r^2 \rho, \quad (3)$$

where P is the pressure, ρ is the density, $M(r)$ is the mass enclosed within radius r , and G is the gravitational constant ($6.67 \times 10^{-11} \text{ m}^3 \cdot \text{kg}^{-1} \cdot \text{s}^{-2}$).

Assuming the polytropic relation above and introducing the dimensionless variables [1]

$$\rho = \rho_c [D_n(\xi)]^n, \quad (4)$$

$$r = \lambda_n \xi, \quad (5)$$

where ρ_c is the central density, D_n is the dimensionless density, ξ is the dimensionless independent variable, and λ_n is a characteristic length scale defined by [1]

$$\lambda_n = \left[(n+1) \left(\frac{K \rho_c^{1-n/n}}{4\pi G} \right) \right]^{1/2}. \quad (6)$$

The equations of stellar structure (Eqs.(2) and (3)) can be combined to yield the Lane-Emden equation [1]:

$$\frac{1}{\xi^2} \frac{d}{d\xi} \left[\xi^2 \frac{dD_n}{d\xi} \right] + D_n^n = 0. \quad (7)$$

In this study, we numerically solve the Lane-Emden equation for selected values of the polytropic index n and analyze the corresponding dimensionless density distributions $D_n(\xi)$. Analytical solutions exist only for $n = 0, 1$, and 5 [1]; therefore, for other values of n , the equation must be solved numerically. The numerical solutions are obtained using a fourth-order Runge-Kutta method [3], and the resulting dimensionless density ratio $\rho/\rho_c = D_n^n$ is plotted as a function of the dimensionless radius $\xi = r/\lambda_n$. The results illustrate how the internal density structure and stellar radius depend on the polytropic index.

II. NUMERICAL METHOD

This section outlines the procedure for numerically solving the Lane-Emden equation (Eq. (7)).

In order to solve a differential equation, we need boundary and initial conditions. For this particular equation (Eq.(7)), the boundary conditions are given by Eqs. (8) and (9) [1]:

$$D_n(\xi_1) = 0, \quad (8)$$

where ξ_1 specifies the surface of the star,

$$\frac{dD_n}{d\xi} = 0 \text{ at } \xi = 0. \quad (9)$$

This condition is derived from the combination of Eqs. (1) and (2) at the center of the star.

Additionally, in order for ρ_c to represent the central density of the star, it is also necessary that [1]

$$D_n(0) = 1. \quad (10)$$

As has been mentioned before, in this study, the Lane-Emden equation was solved numerically using the fourth-order Runge-Kutta method.

To avoid the singularity at the stellar center ($\xi = 0$), the integration starts from a small, finite value ξ_0 , which is set equal to the step size h in the numerical implementation. At ξ_0 , the initial values of D_n and $dD_n/d\xi$ are approximated from the series expansion as [4]:

$$D_n(\xi_0) = 1 - \frac{\xi_0^2}{6}, \quad (11)$$

$$\frac{dD_n}{d\xi} = -\frac{\xi_0}{3}. \quad (12)$$

These expressions ensure that the physical boundary conditions (Eqs. (9) and (10)) are satisfied to first order, providing accurate starting values for the numerical integration. The numerical computations were performed in Python. The integration was carried out up to the first zero of $D_n(\xi)$, with a step size of $h = 0.001$ to ensure numerical stability and accuracy.

III. RESULTS AND DISCUSSION

In this section, the numerical solutions of the Lane-Emden equation are presented. The results for $n = 0$ and $n = 1$ are first compared with their analytical forms to validate the numerical method, followed by the analysis of the solutions for $n = 1.5$ and $n = 3$, which correspond to realistic stellar models.

A. Code verification

Before applying the numerical method to the cases that cannot be solved analytically, the code is first verified by comparing the numerical results with the analytical solutions of the Lane-Emden equation (Eq.(7)) for $n = 0$ and $n = 1$, for which the analytical solutions are available as follows [1]:

$$D_0(\xi) = 1 - \frac{\xi^2}{6}, \quad (13)$$

$$D_1(\xi) = \frac{\sin \xi}{\xi}. \quad (14)$$

Figure 1 shows a comparison between the numerical and analytical solution for $n = 0$, while Figure 2 shows the comparison for $n = 1$. Excellent agreement is observed in both cases, confirming the reliability of the numerical method and justifying its application to polytropic indices without analytical solutions.

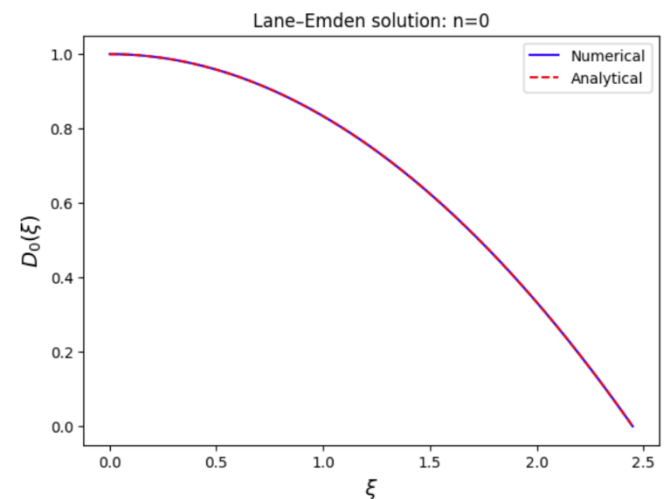


FIGURE 1. Comparison of analytical and numerical solutions for $n = 0$.

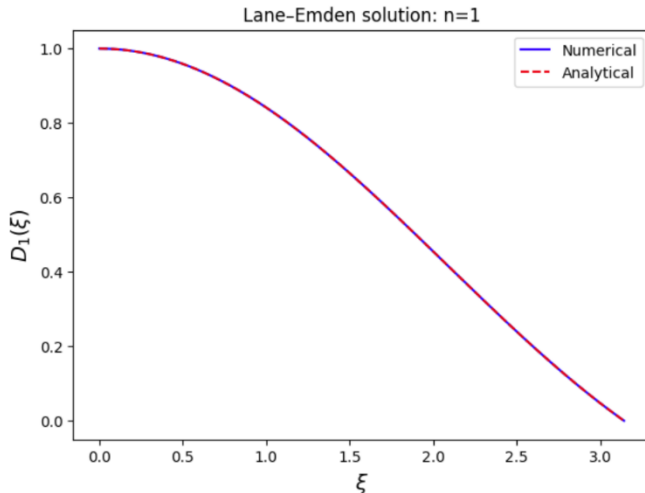


FIGURE 2. Comparison of analytical and numerical solutions for $n = 1$.

B. Density profiles for $n = 1.5$ and $n = 3$

The Lane-Emden equation has been solved numerically for two representative polytropic indices, $n = 1.5$ and $n = 3$, corresponding to distinct stellar configurations. The $n = 1.5$ polytrope characterizes stars supported by non-relativistic degenerate electron pressure, such as white dwarfs—extremely compact remnants in their final evolutionary stage. In contrast, the $n = 3$ polytrope represents stars in radiative equilibrium, where radiation pressure balances gas pressure and gravity, a condition typical of massive main-sequence or radiation-dominated stars [1].

The first zeros of the numerical solutions, which specify the stellar surface, are summarized in Table I. The results indicate that the $n = 1.5$ polytrope corresponds to a more compact configuration, while the $n = 3$ case exhibits a more extended stellar structure.

TABLE I. Dimensionless radii (ξ_1) corresponding to the first zeros of the Lane-Emden function for $n = 1.5$ and $n = 3$.

Polytropic index (n)	ξ_1
1.5	3.654
3	6.897

Figure 3 illustrates the variation of dimensionless density $\rho/\rho_c = D_n^n$ as a function of the dimensionless radius $\xi = r/\lambda_n$ for both values of n ($n = 1.5$ and $n = 3$). In both cases, the density decreases monotonically with increasing ξ . The point where $D_n(\xi)$ first reaches zero, denoted ξ_1 , defines the surface of the star, since beyond this point the density would become negative and thus physically meaningless.

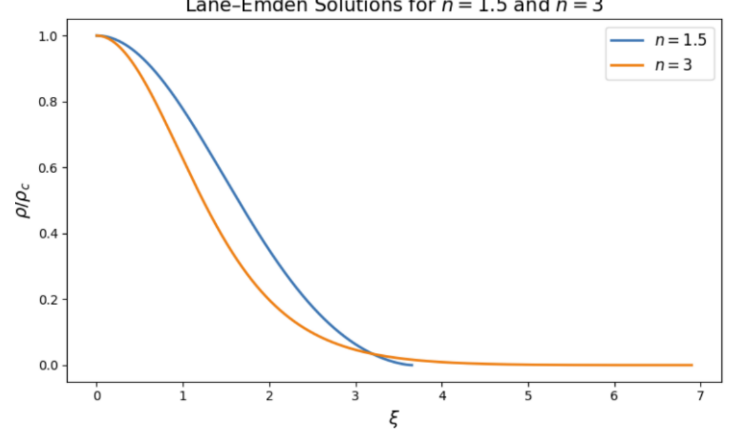


FIGURE 3. Dimensionless density $\rho/\rho_c = D_n^n$ versus dimensionless radius $\xi = r/\lambda_n$ for $n = 1.5$ and $n = 3$

As shown in Figure 3, the $n = 1.5$ density profile declines more steeply and reaches zero at a smaller ξ_1 , indicating a compact star with a centrally concentrated mass. However, the $n = 3$ profile decreases more gradually and extends farther out, representing a radiation-dominated star with a more diffuse structure.

IV. DIMENSIONAL ESTIMATE FOR THE SUN AND COMPARISON WITH OBSERVATIONS

To illustrate how the dimensionless Lane-Emden solution can be converted into a physical stellar radius, we use the $n = 3$ result together with estimates of the solar central pressure and density.

Starting from Eq. (1) and inserting $n = 3$ for the Sun [5] and using $P_c = 2.34 \times 10^{16}$ Pa [1] and $\rho_c = 1.5 \times 10^5$ kg/m³ [6] for the center of the Sun, we have:

$$K = 2.94 \times 10^9 \text{ m}^3 \text{kg}^{-1/3} \text{s}^{-2}. \quad (15)$$

Afterwards, λ_n is calculated from Eq. (6) using ρ_c , $n = 3$, and the value of K from Eq. (15), yielding:

$$\lambda_3 = 7.05 \times 10^4 \text{ km}. \quad (16)$$

Subsequently, substituting calculated λ_3 from Eq. (16) and using ξ_1 from Table I for $n = 3$ in Eq. (5) gives the radius of the Sun as:

$$R_S = 4.87 \times 10^5 \text{ km}. \quad (17)$$

This estimate is of the correct order of magnitude when compared with the observed solar radius $R_\odot = 6.95 \times 10^5$ km [1]. The two-hundred-thousand-kilometre difference is expected given the highly simplified nature of the polytropic model and the approximations used to obtain K .

V. LIMITATIONS OF THE POLYTROPIC MODEL

The difference between the polytropic estimate and the observed solar radius arises from several well-known limitations and approximations:

A. Model assumptions

A single polytropic index n assumes a single power-law relation $P = K\rho^{n+1/n}$ (Eq. (1)) throughout the star. Real stars (including the Sun) are not perfectly polytropic: the inner radiative zone and the outer convective envelope are better represented by different effective indices [4] and by non-polytropic physics.

B. Equation of state simplification

For the Sun we approximated P_c using an ideal-gas relation in order to obtain K . In reality the equation of state varies with depth (partial ionization, radiation pressure, degeneracy in compact objects) [1], so a single K cannot capture the full stratification.

C. Neglected physics

The polytropic Lane–Emden model omits important ingredients: detailed energy generation (nuclear reactions), opacity variations, convective transport, and compositional gradients. These processes affect the pressure and temperature profiles and therefore the mapping between ρ_c , K , and the global radius.

D. Sensitivity to input values

The computed R depends sensitively on the adopted P_c and ρ_c . Small relative uncertainties in those central values produce larger relative changes in K and λ_n because of the power-law dependences.

VI. CONCLUSIONS

In this study, the Lane–Emden equation was numerically solved for several values of the polytropic index using a fourth-order Runge–Kutta method to investigate the internal structure of polytropic stellar models. The numerical solutions were first validated against analytical cases for $n = 0$ and $n = 1$, showing excellent agreement. For the

physically relevant indices $n = 1.5$ and $n = 3$, corresponding respectively to non-relativistic degenerate stars and radiation-dominated stars, the resulting dimensionless density profiles revealed distinct structural behaviors: the $n = 1.5$ polytrope exhibits a compact, centrally concentrated configuration, whereas increasing the polytropic index to $n = 3$ produces a more extended and less centrally condensed stellar model. This general trend reflects the fact that higher polytropic indices correspond to stars with weaker central concentration and broader density distributions.

Applying the $n = 3$ polytropic model to the Sun yielded a stellar radius of the correct order of magnitude compared with the observed value, confirming the usefulness of the Lane–Emden approach as an approximate but insightful tool for modeling stellar interiors. The discrepancies between the model and the actual solar parameters arise from simplifying assumptions in the polytropic equation of state and the neglect of detailed radiative, convective, and compositional effects. Overall, the results demonstrate that the Lane–Emden framework provides a valuable foundation for understanding how the polytropic index governs stellar structure and serves as a baseline for more realistic stellar evolution models.

ACKNOWLEDGEMENTS

The author gratefully acknowledges the academic environment and resources provided by Department of Physics and Energy Engineering.

REFERENCES

- [1] Carroll, B. W. and Ostlie, D. A., *An Introduction to Modern Astrophysics*, 2nd ed. (Pearson/Addison-Wesley, San Francisco, 2007), 1358 pp.
- [2] Chandrasekhar, S., *An Introduction to the Study of Stellar Structure* (Dover Publications, New York, 1957), 509 pp.
- [3] Potter, D., *Computational Physics* (Wiley, New York, 1973), 361 pp.
- [4] Horedt, G. P., *Polytropes: Applications in Astrophysics and Related Fields* (Kluwer Academic Publishers, Dordrecht, 2004), 410 pp.
- [5] Sedek, A., El Sherbini, M., and Osman, M., “Composite Polytropic Models of the Sun,” *ResearchGate Preprint* (2016). Available in: https://www.researchgate.net/publication/335276380_COMPOSITE_POLYTROPIC_MODELS_OF_THE_SUN.
- [6] NASA, “Sun Facts.” Available in: <https://science.nasa.gov/sun/facts/> (visited in October 31, 2025).